

## Near-infrared extinction in the Coalsack Globule 2

Takahiro Naoi<sup>1</sup>, Motohide Tamura<sup>2</sup>, Tetsuya Nagata<sup>3</sup>, Yasushi Nakajima<sup>2</sup>, Hiroshi Suto<sup>2</sup>, Koji Murakawa<sup>4</sup>, Ryo Kandori<sup>2</sup>, Sho Sasaki<sup>5</sup>, Shogo Nishiyama<sup>2</sup>, Yumiko Oasa<sup>6</sup>, and Koji Sugitani<sup>7</sup>

### ABSTRACT

We have conducted  $J$ ,  $H$ , and  $K_S$  imaging observations for the Coalsack Globule 2 with the SIRIUS infrared camera on the IRSF 1.4 m telescope at SAAO, and determined the color excess ratio,  $E_{J-H}/E_{H-K_S}$ . The ratio is determined in the same photometric system as our previous study for the  $\rho$  Oph and Cha clouds without any color transformation; this enables us to directly compare the near-infrared extinction laws among these regions. The current ratio  $E_{J-H}/E_{H-K_S} = 1.91 \pm 0.01$  for the extinction range  $0.5 < E_{J-H} < 1.8$  is significantly larger than the ratios for the  $\rho$  Oph and Cha clouds ( $E_{J-H}/E_{H-K_S} = 1.60\text{--}1.69$ ). This ratio corresponds to a large negative index  $\alpha = 2.34 \pm 0.01$  when the wavelength dependence of extinction is approximated by a power law  $A_\lambda \propto \lambda^{-\alpha}$ , which might indicate little growth of dust grains, or larger abundance of dielectric non-absorbing components such as silicates, or both in this cloud. We also confirm that the color excess ratio for the Coalsack Globule 2 has a trend of increasing with decreasing optical depth, which is the same trend as the  $\rho$  Oph and Cha clouds have.

*Subject headings:* dust, extinction — ISM: globules — ISM: individual (Coalsack)

---

<sup>1</sup>ISAS, JAXA, 3-1-1 Yoshinodai, Sagami-hara-shi, Kanagawa 229-8510, Japan

<sup>2</sup>NAOJ, NINS, 2-21-1 Osawa, Mitaka-shi, Tokyo 181-8588, Japan

<sup>3</sup>Department of Astronomy, Kyoto University, Kitashirakawa-Oiwake-cho, Sakyo-ku, Kyoto 606-8502, Japan

<sup>4</sup>Max-Planck-Institut für Radioastronomie, Auf dem Hügel 69, D-53121 Bonn, Germany

<sup>5</sup>NAOJ, NINS, 2-12 Hoshigaoka, Mizusawa-shi, Iwate 023-0861, Japan

<sup>6</sup>Graduate School of Science and Technology, Kobe University, 1-1 Rokkodai, Nada-ku, Kobe 657-8501, Japan

<sup>7</sup>Graduate School of Natural Sciences, Nagoya City University, Mizuho-ku, Nagoya 467-8501, Japan

## 1. Introduction

Precise determination of the wavelength dependence of extinction is necessary to understand the properties of interstellar dust because differences in the extinction law are attributed to a variation in the dust grains. Differences in extinction laws among various lines of sight throughout the optical and UV properties of the spectrum are widely accepted (e.g., Fitzpatrick 1999). The existence of a corresponding variation at somewhat longer wavelengths is a controversial issue (Whittet 1988; Mathis 1990; Kenyon et al. 1998). For near-infrared wavelengths, recent studies (e.g., Messineo et al. 2005, Nishiyama et al. 2006) have found that the extinction law seems to change from one line of sight to another. These results indicate that the so-called universality (e.g., Mathis 1990) does not necessarily hold for infrared wavelengths.

The color excess ratio,  $E_{J-H}/E_{H-K_S}$ , is one of the simplest parameters available to express the near-infrared extinction law, which can be determined only from  $J$ ,  $H$ , and  $K_S$  photometric observations. In the observations, however, different photometric systems and transformation between them can cause difficult problems in comparing the extinction laws in different regions. Naoi et al. (2006) have shown that the photometry transformation between different photometric systems does not reproduce the real color excess ratio probably because the transformation is mainly determined from the photometry of intrinsically red stars, not reddened stars. Hence, Naoi et al. (2006) have conducted imaging observations for the  $\rho$  Oph and Cha clouds with the same photometric system, and have not found any significant differences in the extinction law,  $E_{J-H}/E_{H-K_S}$ , between the clouds in contrast to previous works (Kenyon et al. 1998; Gómez & Kenyon 2001). Naoi et al. (2006) have suspected that the apparent difference of the color excess ratio,  $E_{J-H}/E_{H-K_S}$ , was caused by the transformation between different photometric systems, at least for these two dark clouds.

Racca et al. (2002) observed the Coalsack and determined the color excess ratio  $E_{J-H}/E_{H-K} = 2.08 \pm 0.03$ , which is significantly larger than the ratios for other clouds (the mean value of  $1.61 \pm 0.04$ , Whittet 1988). They suggested possible changes in grain chemistry with extinction or star formation activity. Though the color excess ratios for the  $\rho$  Oph ( $1.57 \pm 0.03$ , Kenyon et al. 1998), Cha ( $1.80 \pm 0.03$ , Gómez & Kenyon 2001), and Coalsack (Racca et al. 2002) clouds were all expressed in the same CIT system, the photometric system used in the actual observations are different, and the color transformation between them made the comparison very difficult.

Hence we have conducted  $J$ ,  $H$ , and  $K_S$  imaging observations for the Coalsack Globule 2 (about 3 mag deeper than that of Racca et al. 2002) with the same photometric system (SIRIUS/IRSF) as in Naoi et al. (2006) for the  $\rho$  Oph and Cha clouds, and determined

the color excess ratio  $E_{J-H}/E_{H-K_S}$ . We discuss the extinction law of the Coalsack Globule 2 in addition to the  $\rho$  Oph and Cha clouds (Naoi et al. 2006), and also discuss the grain properties in comparison with extinction model calculations.

## 2. Observations

We acquired  $J$  (1.25  $\mu\text{m}$ ),  $H$  (1.63  $\mu\text{m}$ ), and  $K_S$  (2.14  $\mu\text{m}$ ) images of the Coalsack Globule 2 in March–April 2004 with the Simultaneous Infrared Imager for Unbiased Survey (SIRIUS) on the Infrared Survey Facility (IRSF) 1.4 m telescope at the South African Astronomical Observatory (SAAO) in Sutherland, the Republic of South Africa. Dichroic mirrors enabled simultaneous observations in the three bands (see Nagashima et al. 1999 and Nagayama et al. 2003 for the details on the instrument). The camera is equipped with three 1024 $\times$ 1024 pixel HgCdTe (HAWAII) arrays. The pixel scale of the array was 0".453 pixel<sup>-1</sup>, giving a field of view of 7'.7 $\times$ 7'.7.

We acquired 20 s exposure sets for 3 times. Ten dithered frames were obtained for one set of exposures. Total integration time is 10 minutes for each position. Relative positional offsets of dithering were 20" or 25". Typical seeing conditions were 1".3, 1".2, and 1".1 (FWHM) in the  $J$ ,  $H$ , and  $K_S$  bands, respectively. The observations were made at air masses between 1.0 and 1.5. Dark and twilight flat frames were obtained at the beginning and end of each night. We observed standard stars from the faint near-infrared standard-star catalog of Persson et al. (1998) for photometric calibration on the same night.

The target region encompasses heavily extinguished part of the Globule 2 in Coalsack determined from optical extinction and radio CO maps (Racca et al. 2002; Kato et al. 1999). We also observed a reference region in order to estimate the intrinsic color, which lies very close to the target region and falls in regions of relatively low extinction (Racca et al. 2002). The observed areas are summarized in Table 1.

We used NOAO's Imaging Reduction and Analysis Facility (IRAF)<sup>1</sup> software package to reduce the data. We applied the standard procedures of near-infrared array image reduction, including dark current subtraction, sky subtraction, and flat fielding. Each image, following subtraction of the average dark frame, was divided by the normalized flat-field image. Then the thermal emission pattern, the fringe pattern due to OH emission, and the reset anomaly

---

<sup>1</sup>IRAF is distributed by the National Optical Astronomy Observatory (NOAO), which is operated by the Association of Universities for Research in Astronomy (AURA), Inc., under cooperative agreement with the National Science Foundation.

slope pattern of the HAWAII arrays were corrected for each frame, with subtraction of a median sky frame. Identification and photometry of point sources in the all frames were performed with using the DAOPHOT packages in IRAF. The  $10\sigma$  limiting magnitudes ( $\leq 0.1$  mag) for point sources were  $J \sim 19.0$ ,  $H \sim 18.3$ , and  $K_S \sim 17.0$  mag. We used these point sources in analysis, but the point sources brighter than  $J < 12.0$ ,  $H < 11.0$ , and  $K_S < 10.0$  (less than 1% of the total) were not included in our samples because they were saturated.

### 3. Results and determining of the color excess ratio $E_{J-H}/E_{H-K_S}$

Figure 1 shows  $J - H$  vs.  $H - K_S$  color-color diagrams of point sources for the Globule 2 and the reference region in Coalsack. The photometry data described in this paper is in the SIRIUS/IRSF photometric system because we do not use any transformation equations to other photometric systems for photometry in order to avoid possible sources of errors (Naoi et al. 2006). In Table 1, the numbers of identified point sources are also shown.

In order to determine the color excess ratio,  $E_{J-H}/E_{H-K_S}$ , for the Coalsack Globule 2, we employ the powerful method developed by Kenyon et al. (1998). The method determines the ratio accurately even when a number of PMS stars are present in the sample (Naoi et al. 2006). We assume that the stellar population behind the cloud is identical to the stellar population in the reference region. The point source distribution in a color-color diagram is transformed to the density distribution by a kernel density estimator with the kernel as triweight. Figure 2 shows  $J - H$  vs.  $H - K_S$  density distributions drawn from Figure 1 for the Globule 2 and the reference region in Coalsack. Contours are drawn in a logarithmic scale (the same as for all figures below). These color distributions use a kernel density estimator with a smoothing parameter  $h = 0.2$  to derive the density, which is roughly twice the  $1\sigma$  error of our photometry at the survey limits. The sum of multiplications of the density distributions between the target and reference regions provides the reddening probability distribution, which is defined as the probability of measuring a pair of color excesses,  $E_{J-H}$  and  $E_{H-K_S}$ . Figure 3 shows  $E_{J-H}$  vs.  $E_{H-K_S}$  reddening probability contours for the Coalsack Globule 2. We derive the slopes of the reddening vector, namely the color excess ratio  $E_{J-H}/E_{H-K_S}$ , by tracing the ridge of contours on the reddening probability distribution which is divided into the circular annuli centered on the origin. The slope of the reddening locus  $E_{J-H}/E_{H-K_S}$  is determined by a least-squares fit of a straight line with data having errors in both  $x$  and  $y$  coordinates (see Naoi et al. 2006 for more details). The analysis yields  $E_{J-H}/E_{H-K_S} = 1.91 \pm 0.01$  (for  $0.50 < E_{J-H} < 1.8$ ) in the SIRIUS/IRSF photometric system, and the result is summarized in Table 2. In Figure 3, the enlargement with plots of the ridgeline on contour and the best fit lines for the different extinguished

parts are also shown for clearness.

#### 4. Extinction law in the Coalsack Globule 2

Table 2 shows the compilation of the color excess ratios,  $E_{J-H}/E_{H-K_S}$ , for the Coalsack Globule 2 and for the  $\rho$  Oph and Cha clouds (Naoi et al. 2006). The color excess ratio for the Coalsack Globule 2 ( $1.91 \pm 0.01$ ) is significantly larger than those for the mean values of the  $\rho$  Oph ( $1.65 \pm 0.03$ ) and Cha ( $1.67 \pm 0.01$ ) clouds. Moreover, the value in the Coalsack Globule 2 is higher than those in any sub-regions of the  $\rho$  Oph and Cha clouds. These results indicate that a real variation in the near-infrared extinction law occurs from cloud to cloud (see also, Nishiyama et al. 2006 for the case of the observations toward the Galactic Center). The result in the Coalsack Globule 2 supports the relatively large ratio indicated by Racca et al. (2002). The shape of the extinction curve is frequently characterized by a law of the form  $A_{(\lambda)} \propto \lambda^{-\alpha}$ , where  $\alpha$  is the spectral index for near-infrared extinction (e.g., Draine 2003). A good fit to the curve for  $J$ ,  $H$ , and  $K_S$  bands is obtained with  $\alpha = 2.34 \pm 0.01$  by using the mean effective wavelength of the filters (Nishiyama et al. 2006); this index is very large compared to the values in other regions (e.g., Whittet 1988 shows a mean value of  $\alpha = 1.70 \pm 0.08$ ).

Such a large color excess ratio,  $E_{J-H}/E_{H-K_S}$ , and a large spectral index,  $\alpha$ , in the Coalsack are realized when the upper cutoff of the grain size distribution of radius is kept around  $0.2 \mu\text{m}$ , and also if we assume greater dielectric material ratio. Figure 4 shows the calculations of the color excess ratio and the index  $\alpha$  as a function of the upper cutoff of the grain size distribution of radius,  $a_+$ , and the silicate/graphite ratio in the simple MRN model in Naoi et al. (2006). This may indicate that dust grains in the globule do not grow in size so much compared with the standard grain size  $\sim 0.1 \mu\text{m}$  in diffuse interstellar medium (e.g., Mathis 1977). Also, similar model calculations indicate that non-absorbing dielectric materials such as silicates cause rapidly decreasing extinction towards the longer wavelength, and result in large color excess ratios and large spectral indices because the efficiency of the scattering cross section varies in inverse proportion to the fourth power of the wavelength (Rayleigh scattering, e.g., Bohren & Huffman 1983).

We also confirm a systematic shift in the major axis of the probability contour in Figure 3. The plots of the ridgeline on contour and the best fit lines for the different extinguished parts are also shown in the enlargement. The color excess ratio has a trend of decreasing from  $E_{J-H}/E_{H-K_S} = 2.02\text{--}2.08$  for  $0.5 < E_{J-H} < 1.0$  (solid line) to  $E_{J-H}/E_{H-K_S} = 1.87\text{--}1.91$  for  $1.3 < E_{J-H} < 1.8$  (dashed line). The trend is consistent with those in Naoi et al. (2006) for the  $\rho$  Oph and Cha clouds. Kenyon et al. (1998) suggests that the color

excess ratio in the  $\rho$  Oph cloud decreases from  $E_{J-H}/E_{H-K} = 1.65$  for  $0.3 < E_{J-H} < 0.4$  to  $E_{J-H}/E_{H-K} = 1.56$ – $1.57$  for  $1.5 < E_{J-H} < 1.8$ . Kenyon et al. (1998) also indicates a large color excess ratio  $E_{J-H}/E_{H-K} \sim 2$  for the much weaker extinction range at  $E_{J-H} < 0.2$  in the cloud. They suspect that this change might be statistically insignificant. In our case, however, the larger number of reference sources allows us to determine the ratio more precisely. In order to verify the trend, the color excess ratios are determined for the two groups of the sample areas which are defined by the distance from the center of the Globule 2 in Kato et al. (1999); (a) the “inside” sample (radius  $< 250$  arcsec), and (b) the “outside” sample (radius  $> 250$  arcsec). The results are compiled in Table 2. The color excess ratio for the “inside” sample  $E_{J-H}/E_{H-K_S}(\text{in}) = 2.01 \pm 0.03$  is smaller than that for the “outside” sample  $E_{J-H}/E_{H-K_S}(\text{out}) = 2.50 \pm 0.05$  in the same optical depth range of  $0.7 < E_{J-H} < 1.2$ . The trend of the systematic shift in the major axis of the probability contour in Figure 3 is thus verified. As suggested by Naoi et al. (2006) for the  $\rho$  Oph and Cha clouds, this indicates grain growth with optical depth, toward the inside of the dark cloud, also in the Coalsack Globule 2. Therefore, although the grain size in the Coalsack Globule 2 seems to be small compared with other dark clouds, a slight change in size might be taking place from its periphery to the central region.

## 5. Conclusions

1. We have conducted  $J$ ,  $H$ , and  $K_S$  band imaging observations for the Coalsack Globule 2 with SIRIUS/IRSF 1.4m at SAAO and determined the color excess ratio,  $E_{J-H}/E_{H-K_S}$ , by using the method in Kenyon et al. (1998) and Naoi et al. (2006).
2. The color excess ratio for the Coalsack Globule 2 has a significantly larger value than those for the  $\rho$  Oph and Cha clouds (Naoi et al. 2006). Because of employing the same photometric system, our studies are simple and straightforward in comparison of near-infrared extinction laws.
3. The extinction law for the Coalsack Globule 2 shows a trend that the color excess ratio decreases with increasing optical depth. The trend indicated grain growth inside of the cloud, consistent with the results in Naoi et al. (2006) for the  $\rho$  Oph and Cha clouds.
4. The large color excess ratio for the Coalsack Globule 2 could be attributed to small grain growth and grain composition differences.

We are grateful to the SIRIUS/IRSF and SAAO staff, Yoshifusa Ita, Noriyuki Matsunaga, Yoshikazu Nakada, Toshihiko Tanabé, and Cynthia Strydom for their help in support

of observations. T.N. are also grateful to Koji Kawabata for the calculation of extinction, and University of Tokyo, NAOJ, and ISAS/JAXA staffs for support and assistance in this study. We wish to thank the anonymous referee and editors for careful comments. This work is supported by grants-in-aid from the Japanese Ministry of Education, Science, and Culture (Nos. 12309010, 16340061, 16077204, and 15340061).

## REFERENCES

- Bohren, C. F., & Huffman, D. R. 1983, *Absorption and Scattering of Light by Small Particles*, Wiley, New York
- Draine, B. T. 2003, *ARA&A*, 41, 241
- Fitzpatrick, E. L. 1999, *PASP*, 111, 63
- Gómez, M., & Kenyon, S. J. 2001, *AJ*, 121, 974
- Kato, S., Mizuno, N., Asayama, S., Mizuno, A., Ogawa, H., & Fukui, Y. 1999, *PASJ*, 51, 883
- Kenyon, S. J., Lada, E. A., & Barsony, M. 1998, *AJ*, 115, 252
- Mathis, J. S. 1990, *ARA&A*, 28, 37
- Mathis, J. S., Rumpl, W., & Nordsieck, K. H. 1977, *ApJ*, 217, 425
- Messineo, M., Habing, H. J., Menten, K. M., Omont, A., Sjouwerman, L. O., & Bertoldi, F. 2005, *A&A*, 435, 575
- Nagashima, C., et al. 1999, *Star Formation 1999*, ed. T. Nakamoto (Nobeyama: Nobeyama Radio Obs.), 397
- Nagayama, T., et al. 2003, *Proc. SPIE*, 4841, 459
- Naoi, T., et al. 2006, *ApJ*, 640, 373
- Nishiyama, S. et al. 2006, *ApJ*, 638, 839
- Persson, S. E., Murphy, D. C., Krazeminski, W., Roth, M., & Rieke, M. J. 1998, *AJ*, 116, 2475
- Racca, G., Gómez, M., & Kenyon, S. 2002, *AJ*, 124, 2178

Whittet, D. C. B. 1988, *Dust in the Universe*, Cambridge University Press, 25



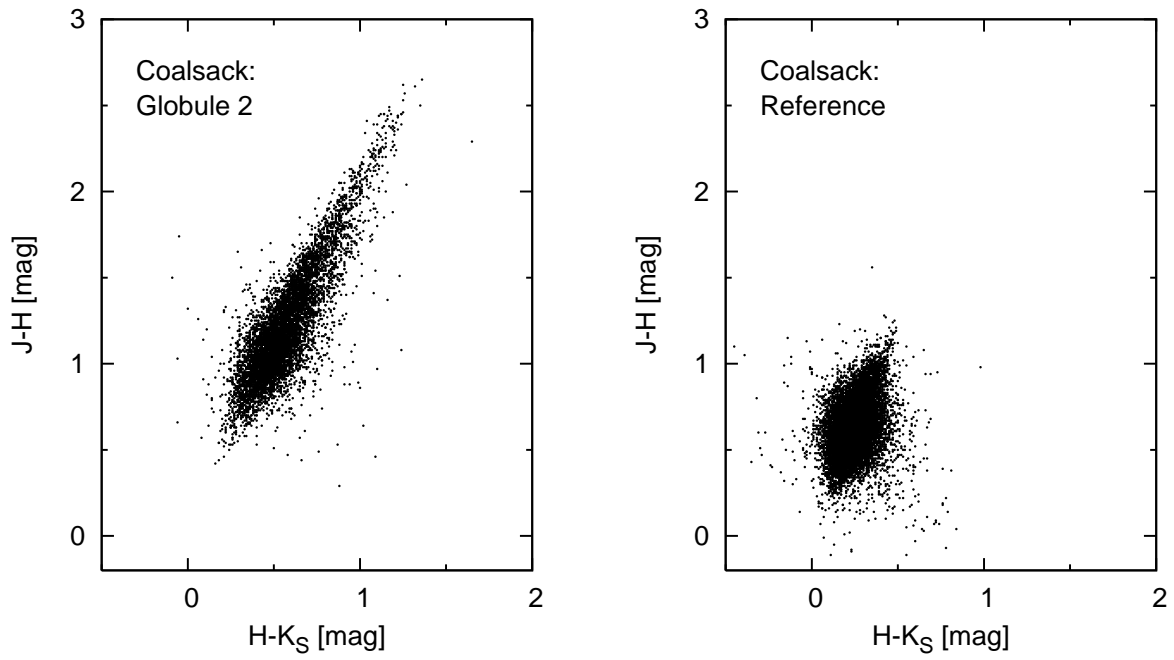


Fig. 1.—  $J - H$  vs.  $H - K_S$  color-color diagrams of point sources for the Globule 2 and the reference region in Coalsack.

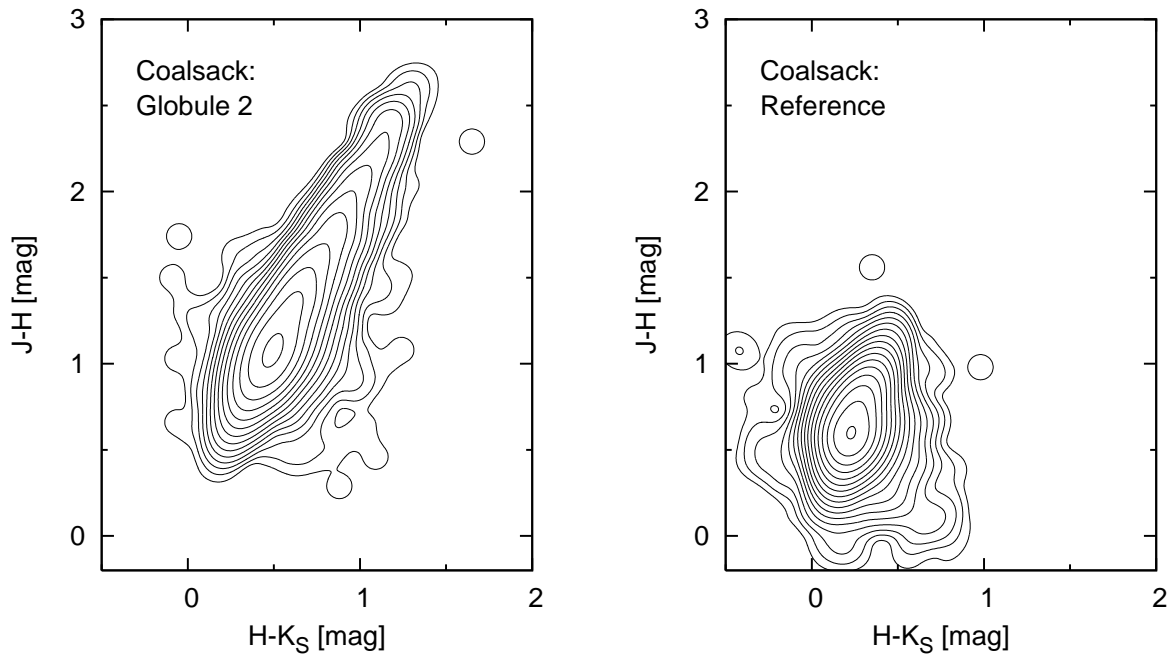


Fig. 2.—  $J - H$  vs.  $H - K_S$  density distributions drawn from Fig.1 for the Globule 2 and the reference region in Coalsack.

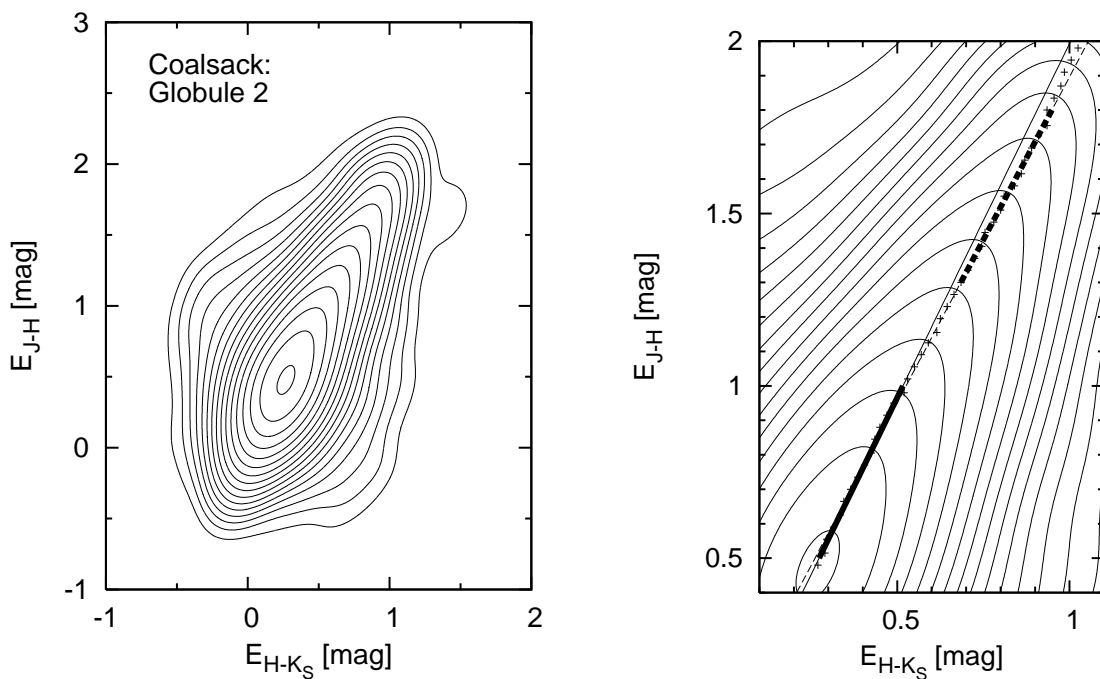


Fig. 3.—  $E_{J-H}$  vs.  $E_{H-K_S}$  reddening probability contour for the Coalsack Globule 2 and the enlargement. The plots of the ridgeline on contour (cross marks) and the best fit lines  $E_{J-H} = 2.05E_{H-K_S} - 0.06$  (for  $0.5 < E_{J-H} < 1.0$ ; solid line) and  $E_{J-H} = 1.89E_{H-K_S} + 0.01$  (for  $1.3 < E_{J-H} < 1.8$ ; dashed line) are also shown in the enlargement. The bold parts of the lines correspond to the fit ranges of the ridgeline.

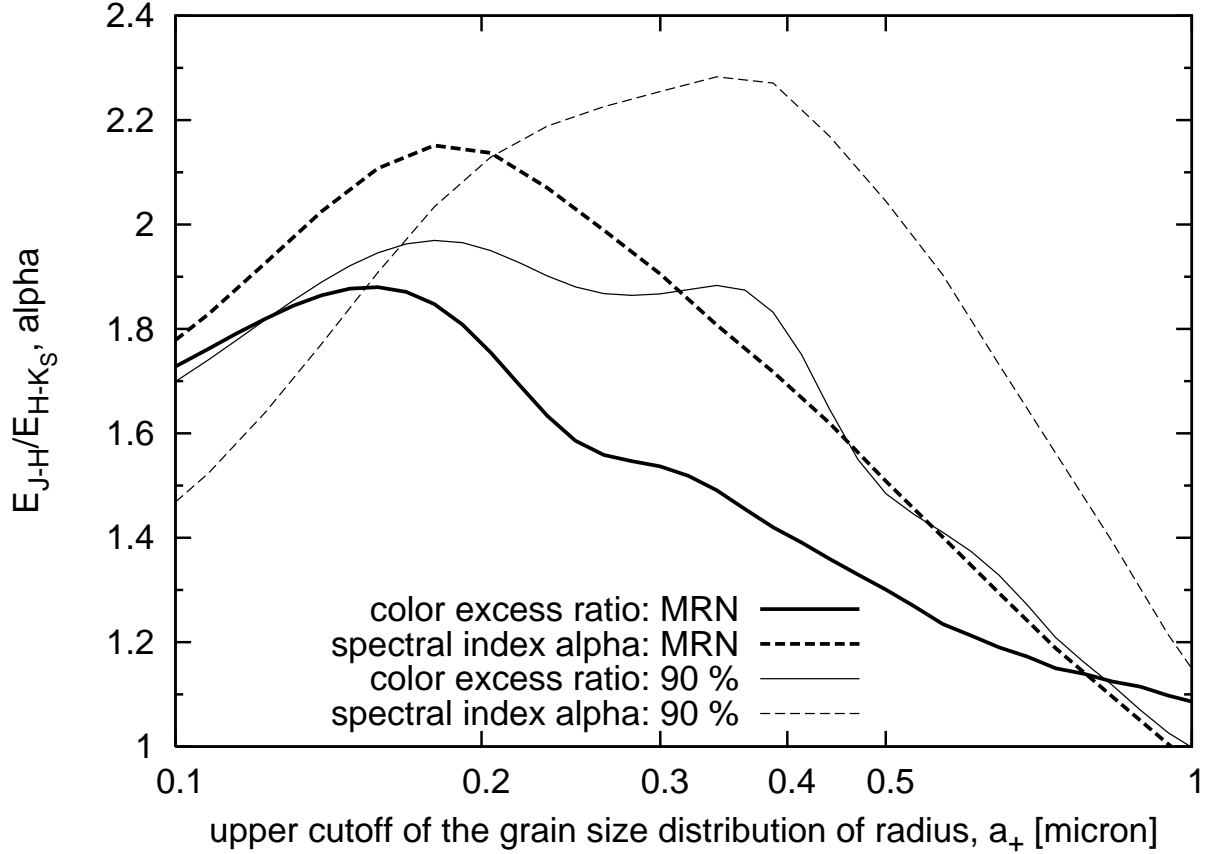


Fig. 4.— Model calculations of the color excess ratio,  $E_{J-H}/E_{H-K_S}$  (solid curves) and the spectral index,  $\alpha$  (dashed curves) as a function of the upper cutoff of the grain size distribution of radius,  $a_+$ , for the different silicate/graphite ratios in MRN (53/47; bold curves) and 90 % (90/10; fine curves). The large color excess ratio and spectral index in the Coalsack can be produced by increasing the abundance ratio of the silicate grain which is the representative material of non-absorbing grains. Spectral index  $\alpha$  is fitted for the mean effective wavelengths of the  $J$ ,  $H$ , and  $K_S$  bands in the SIRIUS/IRSF photometric system (Nishiyama et al. 2006).

Table 1: Center coordinates (J2000.0) of the target and reference regions and the number of identified point sources.

Region	R.A., Dec.	Number
Globule 2	12 31 24, -63 45 11 (10'0 × 10'0)	7236
Reference	12 33 20, -64 24 39 (12'0 × 12'0)	15679

Table 2: Determined color excess ratios,  $E_{J-H}/E_{H-K_S}$ , for the Coalsack Globule 2 with the  $\rho$  Oph and Cha regions<sup>a</sup> (SIRIUS/IRSF photometric system).

Region	$E_{J-H}/E_{H-K_S}$	Range ( $E_{J-H}$ )
Coalsack Globule 2	$1.91 \pm 0.01$	0.50–1.80
	$2.01 \pm 0.03$	0.70–1.20
	$2.50 \pm 0.05$	0.70–1.20
$\rho$ Oph	$1.60 \pm 0.01$	0.50–2.35
	$1.66 \pm 0.01$	0.50–1.70
	$1.68 \pm 0.01$	0.50–1.50
Cha	$1.69 \pm 0.01$	0.50–2.00
	$1.66 \pm 0.01$	0.50–1.80
	$1.67 \pm 0.02$	0.50–1.30

<sup>a</sup>The color excess ratios  $E_{J-H}/E_{H-K_S}$  for the  $\rho$  Oph and Cha clouds are from Naoi et al. (2006)

<sup>b</sup>The samples of the “inside” group are selected by the distance (radius < 250 arcsec, the number of point sources is 3248) from the center coordinate in Kato et al. (1999). The samples of the “outside” are all the other point sources except for the “inside” samples (the number of point sources is 3988).